DOI: 10.21062/mft.2023.104 http://www.journalmt.com

FEM Simulation of the Flange Turning in the Production of Aluminium Aerosol Cans

Csaba Felhő (0000-0003-0997-666X), István Sztankovics (0000-0002-1147-7475), Zsolt Maros (0000-0001-5029-3559), Krisztina Kun-Bodnár (0000-0003-1904-4479)
Institute of Manufacturing Science, University of Miskolc. Egyetemváros, 3515 Miskolc. Hungary. E-mail: csaba.felho@uni-miskolc.hu, istvan.sztankovics@uni-miskolc.hu, zsolt.maros@uni-miskolc.hu, krisztina.bodnar@uni-miskolc.hu

Even today, there is an ever-increasing demand for the production of aerosol cans made of aluminium, as the cosmetics and other propellant-enriched products stored in them reach more and more people with the development of humanity. The production of these packaging materials is primarily carried out by plastic forming operations. However, during the production process of aluminium aerosol cans, tools with a defined edge geometry also perform cutting operations. The processes taking place here affect the quality of the final product. In this paper, the procedure and results of finite element modelling of the flange turning of aluminium aerosol cans is presented. The structure of the finite element model is introduced, as well as the possibilities of considering the peculiarities of the process. Since the used pure aluminium (Al99.5) is considered a difficult-to-cut material, the machinability of aluminium and its alloys is also discussed.

Keywords: aerosol can, aluminium, flange turning, finite element simulation.

1 Introduction

Aluminium aerosol cans, as metal packagings, are produced in a wide variety of sizes and shapes, depending on the materials to be packaged and market needs [1]. In terms of their shape, these bottles are - typically - rotationally symmetrical, and their surfaces are painted and lacquered. The most important operations of aluminium aerosol bottle production [2]:

- Lubrication of aluminium discs;
- Backward impact extrusion (plastic cold forming);
- Trimming (cutting the formed workpieces to size);
- Washing (cleaning);
- Painting and lacquering;
- Necking by rolling and turning;
- Quality inspection;
- Packaging.

As it can be seen from the above operation list, the production of aluminium cans is basically done by different cold plastic forming processes (where untraditional processes can also be applied, like the cold blow forming [3]), but in some cases it is also necessary to cut the cans in different states [4]. A typical such operation is the turning of can flanges shaped by rolling (necking), here the cutting operation is used to finish the connecting surfaces of the flange. In this case, either a flat surface perpendicular to the axis of rotation of the can or a tapered surface at an angle to it is created on the rolled flange. The length of the can is also set with a cutting operation after necking, thereby eliminating the unevenness of length created during necking, and reducing the increased wall thickness caused by clogging. In the current investigations, the turning process of the flat surface on the rolled edge of the can with a design perpendicular to the axis was analysed for the cylinder shown in Fig. 1, where the red line shows the position of the machined surface.

The necking and rolling operation of the can production is carried out on the revolver system equipment developed for this type of operation. In the examined case it was a thirty-position equipment. Unfortunately, we cannot specify the specific machine type here, but practically all machines work on a similar principle. The main component of the equipment is the clamping drum designed to grip the bottles (the workpieces) and performing an intermittent rotating movement. The tool drum equipped with forming tools performing alternating movements. The workpiece pockets of the clamping drum are high-precisely aligned with the pockets of the tool drum that receive the tools. In accordance with the technological sequence, the tools of the various operating elements are attached to the tool drum one after the other. The bottle arriving on the necking device on a conveyor belt is pushed by the feeding unit into the open cartridge of the clamping

pocket of the intermittently rotating revolver drum. When the drum is moved, the chuck closes and remains closed until the last work station. During the further steps, the gripped can body passes in front of the tools of the revolver workstations, and in each position, the corresponding forming step is performed by the forward movement of the tool drum. In the final step, the chuck opens and the ejector removes the finished aerosol can from the chuck, which is transported by the conveyor belt to the next operation site.

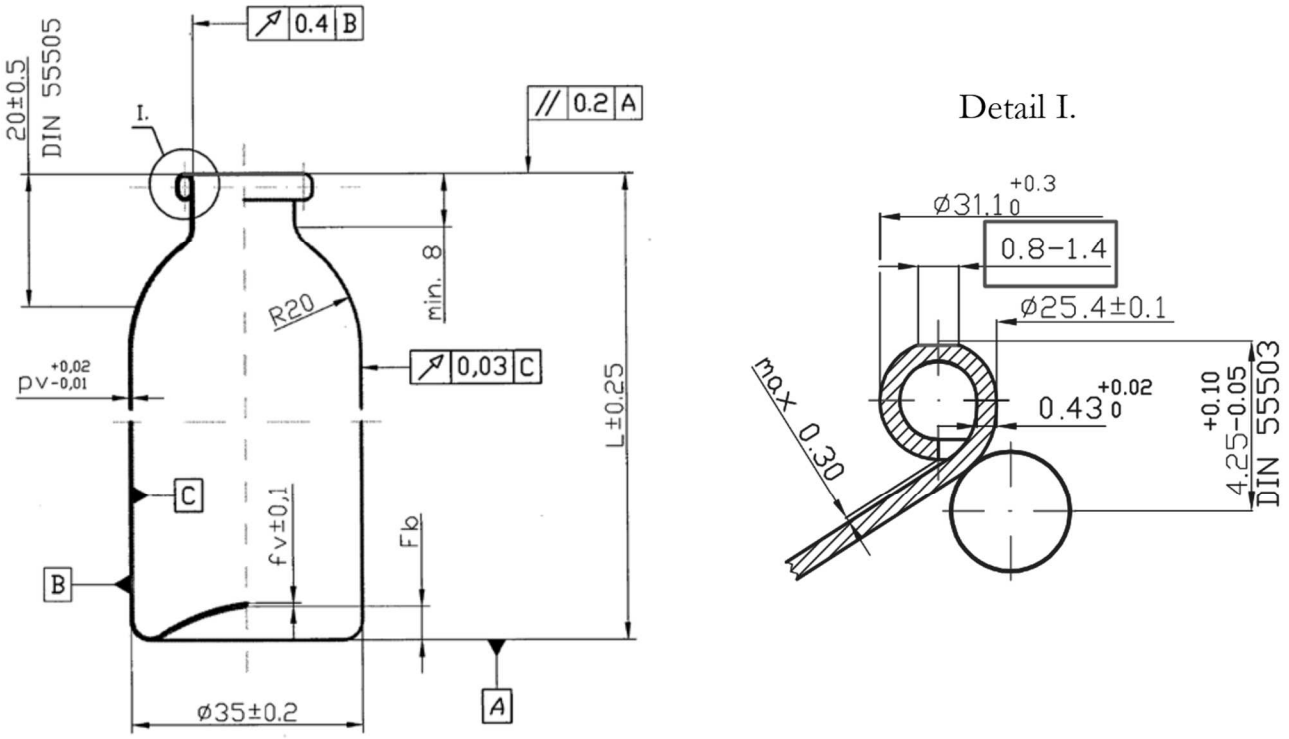

Fig. 1 *Turning the flange of the can by forming a flat surface perpendicular to the can axis*

The difficulties of the cutting process can be traced back to two reasons in aluminium aerosol can production: on the one hand, the necking machine is primarily designed for plastic forming, cutting can be considered an supplementary operation on it, therefore the cutting conditions are not optimal. This will be discussed later. On the other hand, the material used is usually pure aluminium (99.5 or 99.7 grade), which is much more difficult to cut than aluminium alloys. The mechanical properties of the common materials for aerosol cans are summarized in Table 1. In the present investigations, Al99.5 was used, which is highlighted in the table. In the following, the machinability of aluminium and its alloys will be analyzed.

Tab. 1 *Mechanical properties of standard aluminium alloys for aerosol cans [2]*

Mechanical properties					
Alloy	**Hardness ($HB_{2.5/15.625}$)**	**R_m (MPa)**	**$R_{p0.2}$ (MPa)**	**Elongation (%)**	**Grain number/mm²**
99.7	18.5	70	34	42	60-100
99.5	19.5	75	37	41	60-100
AlMn0.3	22	80	41	40	20-30
AlMn0.6	27	92	55	38	30-60

2 Specifics of aluminium machining

Aluminium is used in a wide range of applications [5], including: construction, containers and packaging, material handling, automotive, electronics, consumer durables, machinery and equipment, mirrors, etc. In the food and pharmaceutical industries, as well as in various household products, it is the preferred raw material because it is non-toxic, corrosion-resistant, insoluble and does not splinter when broken. It also reduces bacterial growth and forms colourless salts. Household products made of aluminium are characterised by low weight and a pleasant appearance, and can be shaped into a variety of forms.

These properties make it a suitable raw material for the production of aerosol cans. The machinability of aluminium is generally considered to be good. However, there are differences in machining characteristics between products of different material grades produced by different prefabrication methods, which may require special tooling and processes.

In terms of the manufacturing process of aluminium products, depending on the application, there are many different prefabrication methods [5]. Casting and forging can be used to create prismatic parts with a variety of geometries, while extrusion is the most common method to produce prismatic bars with different sectional geometries. In addition, it can also be used in powder metallurgy. Due to its favourable ductile properties, aluminium is a common raw material for parts to be machined by impact extrusion [6]. In this process, a cold pressing is usually applied to the lubricated preform in the mould, which causes the ductile material to take the desired shape in the gap between the stamp and the pressing tool. This process can be considered a combination of cold forging and cold extrusion [7]. However the stress state of the material must be considered due to its effect on the yield strength [8]. High productivity can be achieved to produce accurate parts of the required quality [9]. For the same reasons, this process is also used for aerosol cans. Among its three variants (forward, backward/reverse and combined extrusion), the products studied in our research are processed by backward extrusion as the first step in the aerosol can manufacturing process.

Among the machining processes, both plastic forming and cutting technologies occur in the production of aluminium products, as is the case with aerosol cans. After creating the desired geometry of the products and flanging, the mouth must be cut to achieve proper connection with the cap to be fitted.

The strength of aluminium and its alloys is low compared to that of other metals, and their thermal characteristics are favorable for processing. Therefore, with the exception of pure aluminium which has high plasticity and toughness, they can generally be machined well [10]. However, Michna et al. also highlighted, that the mechanical properties, mainly the highest elongation, and the other parameters (grain size, metallurgical purity), have an influence on the deep-drawing properties of the sheets [11]. The concept of machinability includes all characteristics related to machining. Thus, in addition to geometric accuracy, the shape of the chip, the cutting forces, the wear of the cutting tool, the roughness and condition of the machined surface are characteristic of the cutting process [12].

Due to their relatively low strength and favorable thermal properties, aluminium alloys can be easily machined, but the machinability of individual alloys is very different [13]. For example, the acting cutting force components are significantly lower than in case of machining of steel workpieces [14]. Among the alloys, those with low hardness (including pure aluminium) can be cut well with a tool with a small tip and edge rounding, even in the case of high-speed steel tool material, at a relatively high cutting speed. However, due to their tendency to "smear", the quality of the machined surface - mainly its roughness - is not satisfactory [15, 16]. The Fig. 2. shows the typical properties of aluminium alloys that affect machinability.

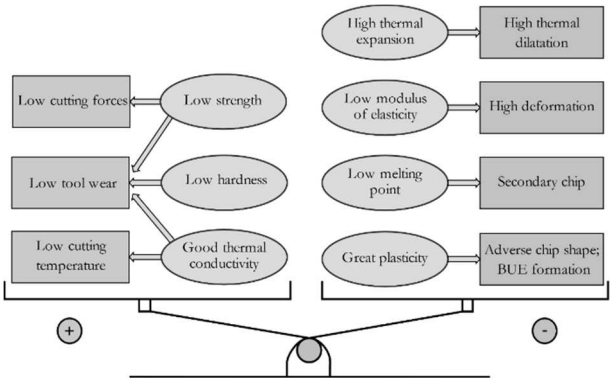

Fig. 2 *Properties of aluminium alloys in terms of machinability*

Pure, unalloyed aluminium is relatively soft and deforms easily, which results a long, ribbon-like chip and a tendency to form Built-Up-Edge (BUE) when it sticks to the cutting tool [17]. It is necessary to use a suitable machining process to avoid rough surface quality and burr formation [5]. The machinability properties of aluminium can be improved by alloying. Materials that make it heat treatable or susceptible to form hardening increase the hardness of the aluminium matrix, thereby reducing edge and burr formation, as well as improving the surface quality, reducing the torn character of the machined surface and the length of the chips produced [18]. This phenomenon is also strengthened by the various undissolved elements, as they act as chip breakers. Among the aluminium alloys with relatively higher hardness, the abrasive effect against the tool can be a problem when cutting [19].

With the right choice of cutting data, the use of cooling-lubricating fluid, modern tools with correct edge geometry and good surface quality, the majority of aluminium materials can be machined well [13]. Since it is characterized by a lower specific cutting force compared to iron-based metal alloys, we can work with higher values in terms of cutting speed than when cutting steels [20]. This is also helped by its low density, as it is therefore less sensitive to dynamic imbalance at high rotation speeds. Due to the abrasive aluminium oxides present in the raw material, this technological parameter can be four to eight times

ISSN 1213–2489
e-ISSN 2787–9402

higher. Here, the lower melting point of aluminium can be an additional upper limit, since this temperature can be reached with incorrectly chosen technological characteristics during chip removal. It is advisable to choose a high value for the feed, similar to the cutting speed, so that the cutting process taking place between the chip and the workpiece does not turn into rubbing. In addition, in the case of the depth of cut, it is customary to choose a larger value compared to that of steels in order to maintain the lower specific load and the correct chip thickness/width ratio.

The high cutting speed helps to reduce the phenomenon of Built-Up-Edge formation [18]. However, the material in contact with the tool (mainly due to friction on the clearance surface) softens due to the temperature and the forming speed, so the pressure can push it out of the contact zone. It then solidifies again, which creates an attached layer on the tool with a hardness similar to that of the chip. This phenomenon causes the workpiece to heat up and deteriorates the surface quality [21]. To avoid this, it is advisable to reduce the contact surfaces to a minimum. However, due to the larger extent of the main cutting motion compared to that of steel, more chips are generated in a unit of time, the proper removal of which requires attention. In order to avoid the chip getting stuck on the workpiece or tool, it is customary to work with tools with a wider chip breaker and a larger cutting edge inclination angle [22], and in the case of tools with multiple edges, it is better to choose a construction with fewer edges. The tool used in the present investigations is an HSS insert bit, and the analyses were aimed at the finite element determination of certain characteristics of the cutting process, based on which conclusions can be made about the machinability of the material and the useability of the tool for that task.

3 Finite element modeling of flange turning

The finite element investigations were performed in the DEFORM 3D software which can be used not only for plastic forming, but also (among many other technologies) for cutting technology modeling [23, 24]. In the following, the process of model creation is briefly described, with the main emphasis being placed on the set parameters. As already mentioned in the introduction, the flange turning is performed on the necking machine, with a cutting tool placed in one of its tool holder pockets. The cutting tool itself, with the insert bits, is mounted on one of the sockets of the forming tool drum of this workstation, together with a motor that rotates the tool as shown in Fig. 3.

Consequently, the feed motion of the tool is provided by the alternating motion of the workpiece drum. The cutting tool works at the end of the stroke, at which point the drum slows down until it comes to a complete stop. Thus, the feed rate (327 mm/s) calculated from the set stroke rate of the drum (120 strokes/min) for the short period of cutting may be much lower than the theoretical value. This should be addressed during the simulation as it will be introduced later.

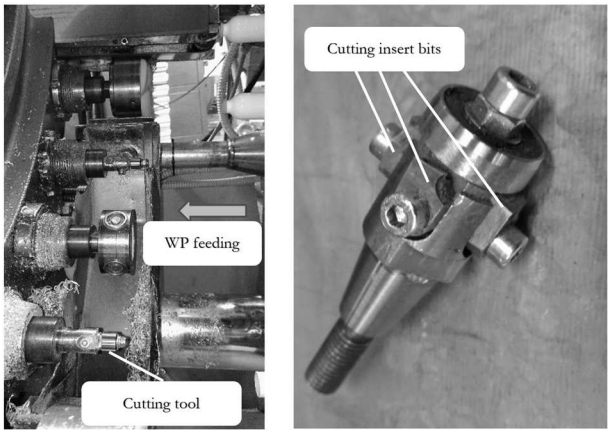

Fig. 3 *Detail of the shaping drum and the cutting tool with cutting bits*

For modeling, it was necessary to determine the actual axial cutting length, the calculation of which can be solved using simple trigonometric relationships from the workpiece geometry shown in Fig. 1. Fig. 4 shows this simple calculation problem, and the calculated value of the feeding motion length is 0.09 mm.

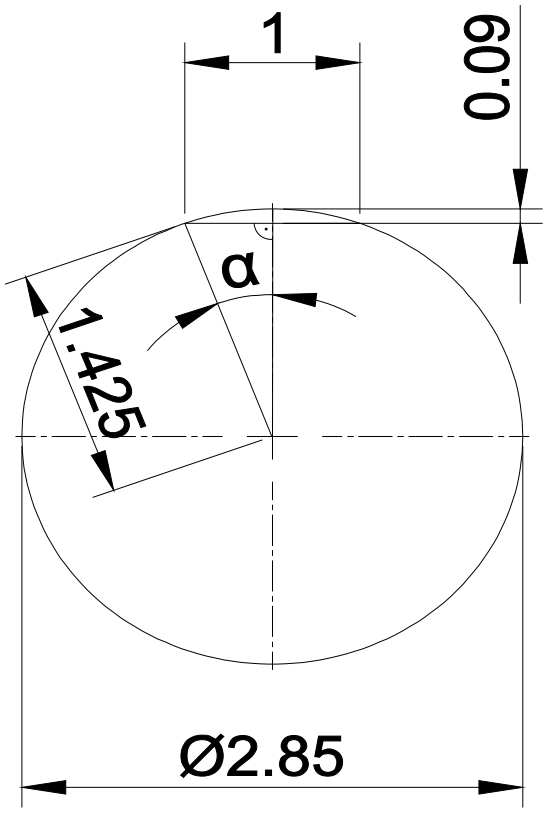

Fig. 4 *Calculation of the cutting length*

indexed on http://www.webofscience.com and http://www.scopus.com

Based on the data received from aeresol can producer company, the rotational speed of the tool is n = 9600 RPM, and the value of the axial speed used is v_f = 327 mm/s, so the value of the feed per revolution is around f ≈ 2 mm/revolution.

First, the geometry of the workpiece was specified, where the entire can was not needed for the simulation, a simplified modeling of the rolled edge (flange or neck) was enough. This was defined by selecting the "Hollow Cylinder" option of the "Geometry Primitive" command in the software.

For the tool, a previously created three-dimensional model was used, converted it into STL format and read it directly into the software. The object type have been set to "Rigid" for the tool, which means that the software will not treat it as a deformable body, and will not calculate any deformations for it. Since the material to be machined is much softer than the high speed steel tool used, this does not represent a big deviation from the real process. Naturally, the "Plastic" object type was used to model the workpiece.

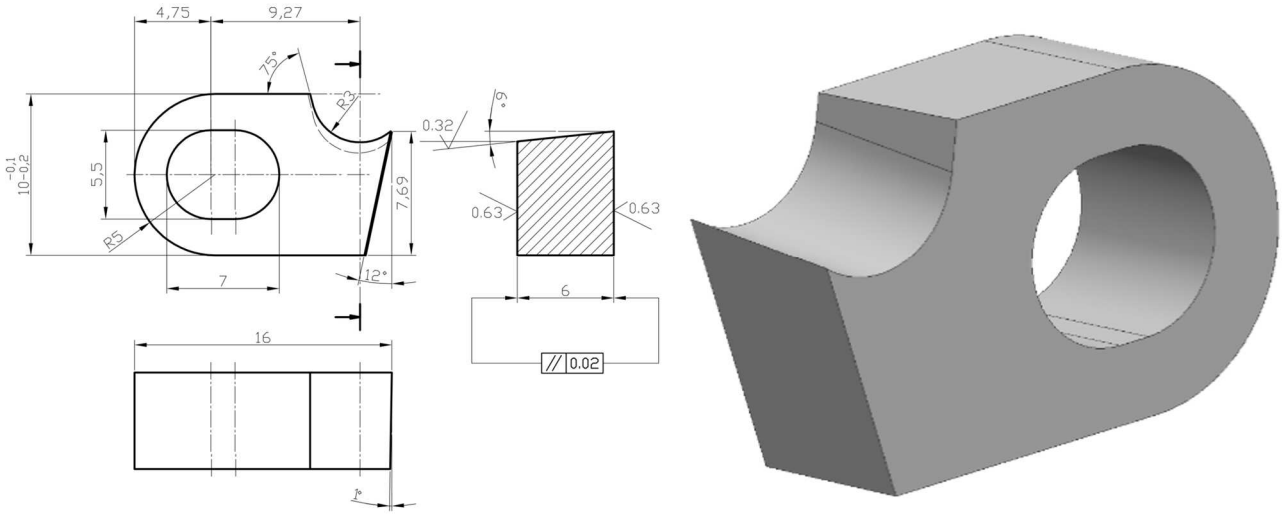

Fig. 5 *Drawing and 3D model of the cutting insert bit*

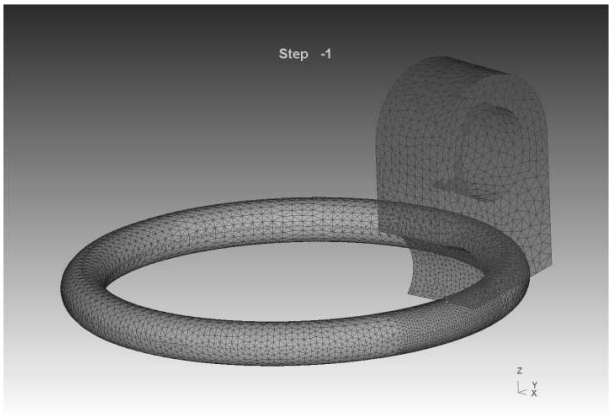

Fig. 6 *Modelling the flange with a ring and the meshing of the workpiece and the tool*

When specifying the material characteristics, the standard properties of the Al99.5 material grade already described in Table 1 were given for the simulation. The next step was to specify the meshing of the workpiece and the tool. In both cases, the geometric elements were meshed in such a way that a denser mesh was used in the vicinity of the cutting zone. In the case of the workpiece, a mesh with many more elements was needed, since the actual deformation and the chip separation will occur in this mesh. So the number of elements on the workpiece was set to 60,000 and in the tool to 20,000, and set it to create a three times denser mesh within a range specified by a cube (which moves with the cutting tool and is the area around the cutting zone) [25]. For the tool, the mesh is only relevant for heat spreading, so a mesh of 20,000 elements was sufficient, but here we also set the system to use a denser mesh in the vicinity of the cutting zone.

As the next step, the movement of the elements during the process was specified: the tool performs the circular movement as well as the feed movement while the workpiece is stationary, so the previously described feed speed and rotational speed values were set for the tool. As a boundary condition, it was specified that the lower part of the ring is fixed, so its velocity is zero in the direction of all three coordinate axes. Since the cutting must take place at the end of the working stroke, the actual feed rate may be much lower than the 327 mm/s given by the company, and in fact it should be zero at the end of the cutting. This is supported by the fact that the thickness of the separated layer is 0.09 mm, while the value of the feed per revolution is 2 mm/revolution with the value of the given feed speed. So, theoretically, to remove the 0.09 mm layer, only 16° angular rotation would be required, if the tool did not stop at the end of the stroke, but could move directly back from maximum

speed. However, this is obviously not the case in reality, but we did not manage to obtain any information about the deceleration and about the actual direction change process. Thus, it was assumed in the software (Fig. 7) that at the beginning of cutting, the tool still moves at full speed at the "zero" moment and from there it slows down uniformly to zero speed until the stroke length of 0.09 mm is reached. From then on, there is no feed, only the main cutting movement, which is the circular movement of the tool on the workpiece; however, chip removal naturally continues until the tool completes one full revolution plus the plunging section.

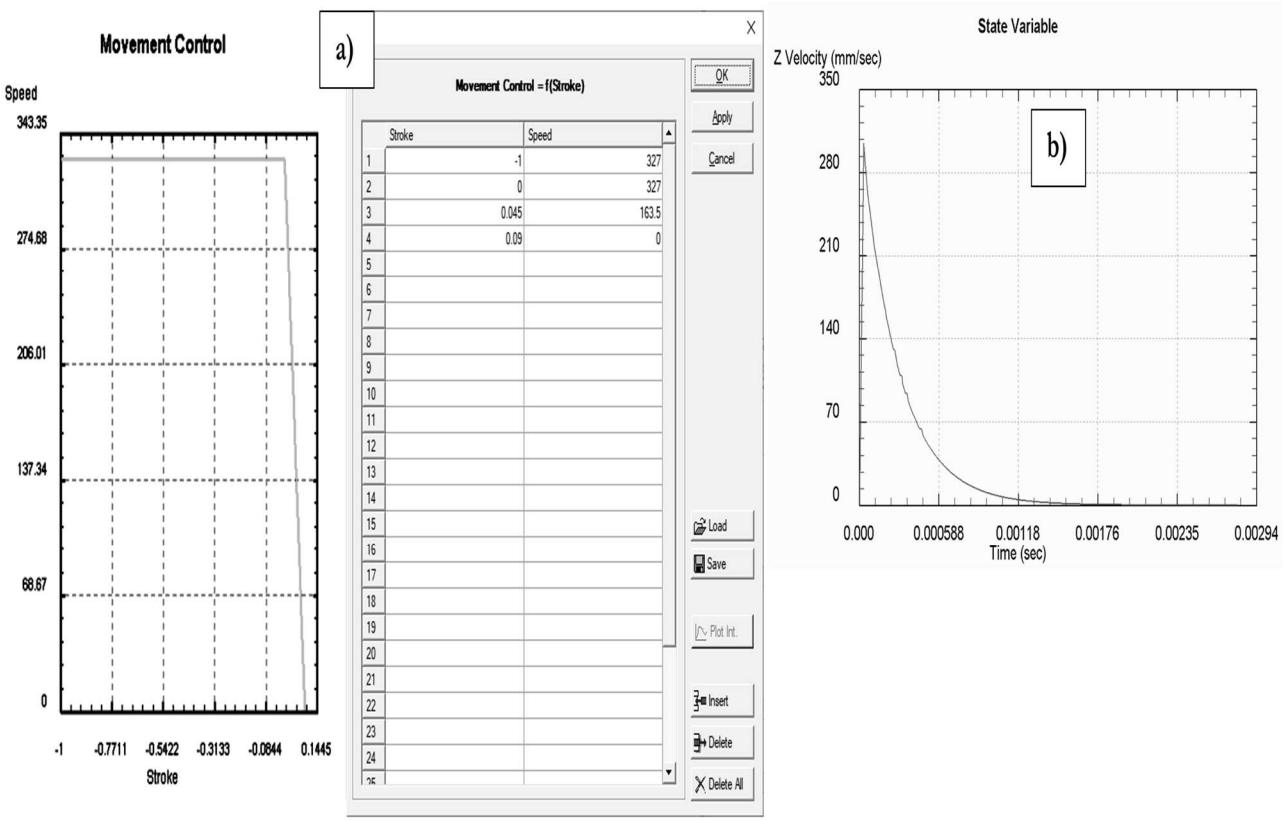

Fig. 7 *Entering the feed rate in the software (a), which decreases as a function of the stroke length and time (b)*

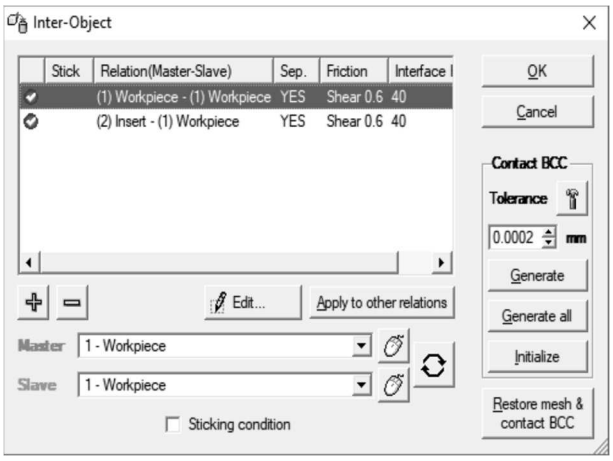

Fig. 8 *Specifying Inter-Object relationships in the simulation*

In the next step, the contact condition between the tool and the workpiece was created, but for this the bodies should be brought into contact with each other, so that the cutting can begin as a result of the specified movement. This can be accomplished using the "Interference" option of the "Object positioning" menu. It was also necessary to specify the connections between the objects ("Inter-Object", see Fig. 7), together with the definition of the friction coefficient (0.6) and the heat transfer coefficient (40 W/m²K). Here, two connections are possible: the tool and the workpiece should be interacted, and the workpiece can also interacts with itself (since a part of it is detached as a chip, and this can also connect to the non-detached part of the material). Then the contact condition between the two bodies was created by using the "Contact BCC" command.

4 Results and discussion

Fig. 9a shows the nature of chip removal. As mentioned earlier, half a tool revolution was simulated during the test, since there are two insert bits in the turning head, so one tool edge must make about half a revolution to form the desired surface.

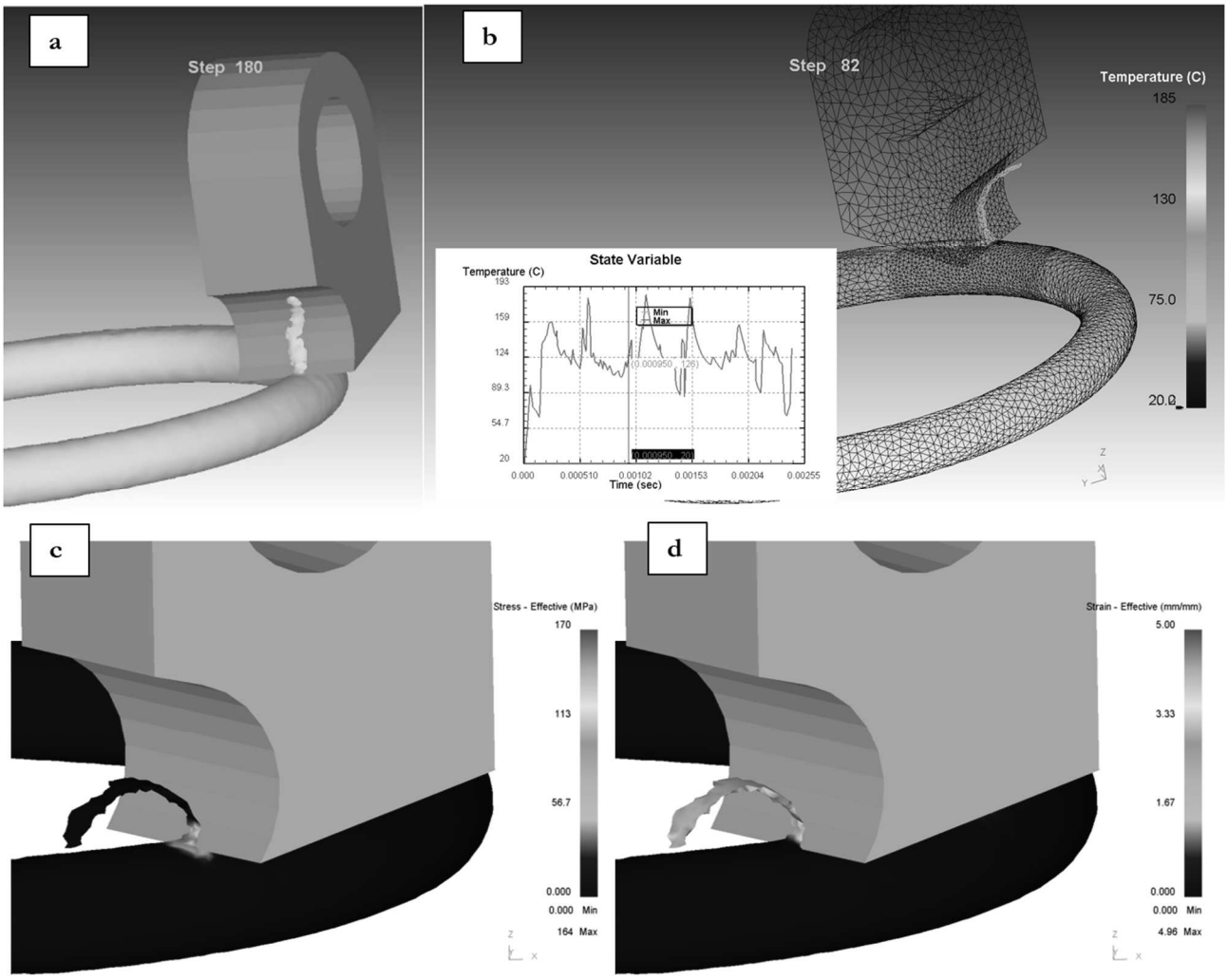

Fig. 9 *Evaluation of stresses and strains during cutting*
(a: Simulation of chip removal; b: Cutting temperature vs. cutting time; c: Stress; d: Effective strain)

A total of five separated pieces of chip were removed from the workpiece during the half-turn, of which in two cases a larger chip came off, while in the other cases it came off the workpiece almost immediately after the chip was formed. Fig. 9b shows the change in temperature. It can be seen that the highest temperature occurs in the chip, the maximum of which is 185 °C, and the average value is around 120 °C.

Fig. 9c shows the effective stresses. Here it can be seen that the maximum of the stresses is found in the removed chip, in the immediate vicinity of the shear plane, the numerical value of which is 164 MPa at the time of cutting shown in the figure. Fig. 9c shows the effective stress; here it can be seen that the maximum of the stress can be found in the chip, again in the immediate vicinity of the shear plane, the numerical value of which is 164 MPa at the shown cutting momentum. Finally, Fig. 9d shows the change in the strain at a given moment of the simulated cutting cycle. The figure indicates that the distribution of the deformation in the chip is almost uniform, and the maximum value is around 5 mm/mm.

5 Conclusions

The production of aluminium aerosol cans consist mainly of forming processess; however, machining with chip removal is also applied among the finishing operations to achieve the prescribed accuracy. Flange turning is a cutting process that lasts for a very short time and takes place with a constantly changing feed, the experimental modeling of which is difficult to implement. That is why it is of great importance that conclusions can be drawn from the results of the finite element analysis. These are the following:

- In the process under study, chip removal is continuous, but the chip breaks, with about five chip breakages in the simulation. Analysing the shape of the chip, it can be concluded that it is certainly favourable that no lumpy chips are produced.

- The maximum temperature during the cutting was 183°C, so high temperatures should not be expected when machining the flange surfaces of aluminium aerosol cans.
- The axial force components are small (52 N maximum) and therefore do not cause significant deformation of the can.
- In terms of stresses and strains, the maximum strain is found to be 5 mm/mm, with a relatively uniform distribution in the chip. The maximum stress in the chip, in the vicinity of the shear plane, was 220 MPa.

Based on all of this, it can be said that the flange turning of Al99.5 aluminium cans is a process with adequate chip removal at low temperatures, with small resultant cutting forces, which ensures the production of the sealing surface on the aerosol can with the appropriate quality. The study will be continued by the analysis of achievable shape accuracy.

References

[1] NIEMIEC, K., FITRZYK, A., GRABOWIK, C. (2021). Methods of manufacture and innovations in steel aerosol cans' production. In: *International Journal of Modern Manufacturing Technologies*. Vol. 13, No. 3, pp. 96–104 DOI: 10.54684/ijmmt.2021.13.3.96.

[2] KORES, S., TURK, J., MEDVED, J., VONČINA, M. (2016). Development of aluminium alloys for aerosol cans. In: *Mater. Tehnol.* Vol. 50, No. 4, pp. 601–605 DOI: 10.17222/mit.2015.330.

[3] GIULIANO, G., PARODO, G., POLINI, W., SORRENTINO, L. (2023). Cold Blow Forming of a Thin Sheet in AA8006 Aluminum Alloy. In: *Manufacturing Technology*. Vol. 23, No. 3, pp. 284–289 DOI: 10.21062/mft.2023.038.

[4] PAGE, B. (2012). Rigid metal packaging. In: *Packaging Technology*. Elsevier. pp. 122–162 ISBN 978-1-84569-665-8.

[5] ASM HANDBOOK COMMITTEE (1990). *ASM Handbook* Vol. *2*: *Properties and Selection: Nonferrous Alloys and Special-Purpose Materials*. ASM International. Novelty, Ohio. p. 3470 ISBN 978-1-62708-162-7.

[6] DESSIE, J.E., LUKACS, Z. (2022). Necking limit analysis of thin wall aerosol can. In: *Pollack Periodica*. Vol. 17, No. 2, pp. 48–53 DOI: 10.1556/606.2022.00558.

[7] KIM, H.-S., RHIM, S.-H., HWANG, J.-I. (2020). Preliminary study of backward impact extrusion process design for aluminum air suspension tube using finite element analysis. In: *Proceedings of the International Conference of Manufacturing Technology Engineers (ICMTE) 2020*. pp. 61–61.

[8] SOBOTKA, J., SOLFRONK, P., KORECEK, D. (2020). Influence of Stress State on the Yield Strength of Aluminium Alloy. In: *Manufacturing Technology*. Vol. 20, No. 1, pp. 92–97 DOI: 10.21062/mft.2020.005.

[9] ORANGI, S., ABRINIA, K., BIHAMTA, R. (2011). Process Parameter Investigations of Backward Extrusion for Various Aluminum Shaped Section Tubes Using FEM Analysis. In: *J. of Materi Eng and Perform*. Vol. 20, No. 1, pp. 40–47 DOI: 10.1007/s11665-010-9655-8.

[10] CARRILERO, M.S., MARCOS, M. (1996). On the Machinability of Aluminium and Aluminium Alloys. In: *Journal of the Mechanical Behavior of Materials*. Vol. 7, No. 3, pp. 179–194 DOI: 10.1515/JMBM.1996.7.3.179.

[11] MICHNA, Š., HREN, I., CAIS, J., MICHNOVÁ, L. (2020). The Research of the Different Properties and Production Parameters having Influence on Deep-Drawing Sheets made of AlMg3 Alloy. In: *Manufacturing Technology*. Vol. 20, No. 3, pp. 347–354 DOI: 10.21062/mft.2020.035.

[12] MILLS, B., REDFORD, A.H. (2011). *Machinability of Engineering Materials*. Springer Netherlands. Dordrecht. p. 174 ISBN 978-94-009-6633-8.

[13] JOEL, J., ANTHONY XAVIOR, M. (2018). Aluminium Alloy Composites and its Machinability studies; A Review. In: *Materials Today: Proceedings*. Vol. 5, No. 5, Part 2, pp. 13556–13562 DOI: 10.1016/j.matpr.2018.02.351.

[14] MAJERÍK, J., DUBOVSKÁ, R., BAŠKA, I., JAMBOR, J. (2018). Experimental Investigation and Measurement of Surface Roughness and Cutting Forces while Turning AlCu3MgMnPb Aluminium Alloy. In: *Manufacturing Technology*. Vol. 18, No. 1, pp. 66–71 DOI: 10.21062/ujep/55.2018/a/1213-2489/MT/18/1/66.

[15] HORVÁTH, R., CZIFRA, Á., DRÉGELYI-KISS, Á. (2015). Effect of conventional and non-conventional tool geometries to skewness and kurtosis of surface roughness in case of fine turning of aluminium alloys with diamond tools. In: *Int J Adv Manuf Technol*. Vol. 78, No.

1–4, pp. 297–304 DOI: 10.1007/s00170-014-6642-5.

[16] LAWAL, S.A., AHMED, A.M., LAWAL, S.S., UGHEOKE, B.I. (2016). Effect of HSS and Tungsten Carbide Tools on Surface Roughness of Aluminium Alloy during Turning Operation. In: *American Journal of Mechanical Engineering*. Vol. 4, No. 2, pp. 60–64 DOI: 10.12691/ajme-4-2-3.

[17] AKKURT, A. (2015). The effect of cutting process on surface microstructure and hardness of pure and Al 6061 aluminium alloy. In: *Engineering Science and Technology, an International Journal*. Vol. 18, No. 3, pp. 303–308 DOI: 10.1016/j.jestch.2014.07.004.

[18] SONGMENE, V., KHETTABI, R., ZAGHBANI, I., KOUAM, J., DJEBARA, A. (2011). Machining and Machinability of Aluminum Alloys. In: *Aluminium Alloys, Theory and Applications*. IntechOpen. London. pp. 377–400 ISBN 978-953-307-244-9.

[19] OKOKPUJIE, I.P. et al. (2017). Experimental and Mathematical Modeling for Prediction of Tool Wear on the Machining of Aluminium 6061 Alloy by High Speed Steel Tools. In: *Open Engineering*. Vol. 7, No. 1, pp. 461–469 DOI: 10.1515/eng-2017-0053.

[20] BÁTORFI, J.G., ANDÓ, M. (2020). Study of Parameters during Aluminum Cutting with Finite Element Method. In: *Period. Polytech. Mech. Eng.* Vol. 64, No. 2, pp. 136–144 DOI: 10.3311/PPme.14641.

[21] ROY, P., SARANGI, S.K., GHOSH, A., CHATTOPADHYAY, A.K. (2009). Machinability study of pure aluminium and Al–12% Si alloys against uncoated and coated carbide inserts. In: *International Journal of Refractory Metals and Hard Materials*. Vol. 27, No. 3, pp. 535–544 DOI: 10.1016/j.ijrmhm.2008.04.008.

[22] ASTAKHOV, V.P. (2010). *Springer Series in Advanced Manufacturing Geometry of Single-point Turning Tools and Drills*. Springer. London. p. 565 ISBN 978-1-84996-052-6.

[23] DAVIM, J.P. ed (2012). *Statistical and Computational Techniques in Manufacturing*. Springer. Berlin, Heidelberg. ISBN 978-3-642-25858-9.

[24] PARIHAR, R.S., SAHU, R.K., SRINIVASU, G. (2017). Finite Element Analysis of Cutting Forces Generated in Turning Process using Deform 3D Software. In: *Materials Today: Proceedings*. Vol. 4, No. 8, pp. 8432–8438 DOI: 10.1016/j.matpr.2017.07.188.

[25] MATHIVANAN, A., SWAMINATHAN, G., SIVAPRAKASAM, P., SUTHAN, R., JAYASEELAN, V., NAGARAJ, M. (2022). DEFORM 3D Simulations and Taguchi Analysis in Dry Turning of 35CND16 Steel. In: *Advances in Materials Science and Engineering*. Vol. 2022, pp. 1–10 DOI: 10.1155/2022/7765343.